

## Optimal Velocity Control Method in Path Following Control Problem

H. Okajima\* T. Asai\*\* S. Kawaji\*\*\*

\* *Kumamoto University, Kurokami, Kumamoto-City, Japan  
(e-mail:okajima@cs.kumamoto-u.ac.jp)*

\*\* *Osaka University, Yamadaoka, Suita-City,  
Japan(e-mail:tasai@mech.eng.osaka-u.ac.jp)*

\*\*\* *Kumamoto University, Kurokami, Kumamoto-City, Japan  
(e-mail:kawaji@cs.kumamoto-u.ac.jp)*

---

**Abstract:** Path following control problem is treated in recent years. In many past results of path following control, it is assumed the plant has single-input and the velocity of the plant is considered as constant value. However, when we have to reduce traveling time, we must control velocity of the plant in tracking problem. In this paper, velocity control and path following task are achieved at the same time by optimal control. To achieve these tasks, we assume multi-input plants are given. Since sum of reaching time and input costs is used as a cost, we can obtain good acceleration and deceleration input. By a constraint for the cost function, the error from the plant to a given reference path goes to zero when time goes to infinity. The effectiveness of the proposed method is examined by numerical examples of an automobile model.

Keywords: Autonomous vehicle; Tracking; Target tracking; Time-optimal control; Boundary value problem.

---

### 1. INTRODUCTION

Path following control problems aim to find control inputs which make automobiles track to given reference paths. These problems have been paid attention and many results have been published ( Sampei et al [1994, 1995], Altafini [2002], Soetanto et al [2003] ).

In many researches of path following problems, the velocity of plants are considered as constant value for ease. However, not only path following but also rapidly moving is required in many actual path following problem such as car racing, ultrafast operation of manipulator. The velocity should be controlled to quicken up when we aim rapidly moving. In contrast, when large input is difficult to input for the plant, we should control the velocity for decelerating to take a short turn ( See, for example, automobile model of Abe [1979] ). Therefore, we should do adequate velocity control based on information of dynamics of the plant and the shape of the reference path. However, velocity control method in path following has not been considered.

In this paper, velocity control method in path following problem is proposed based on optimization control of cost function. The cost functions are used for minimizing traveling time and for achieving small control inputs. To achieve path following, one of control inputs would be constrained based on output-zeroing ( See, for example, Isidori [1995] ). By using the constraint for path following, the plant tracks to the reference path asymptotically.

Velocity of plants has been treated in many researches ( Casanova et al [2001], Rajan [1985], Chen et al [1989],

Galicki [2000], Kaminer et al [2006], Okajima et al [2004] ). However, these researches are not concerned with path following problem. Casanova et al [2001] have analyzed the given data of lateral acceleration and longitudinal acceleration of F1 race car. Velocity is controlled for collision-avoidance in Kaminer et al [2006]. The aim of this method is not time optimization. Not only velocity but also path of the plant are controlled in Rajan [1985], Chen et al [1989], Galicki [2000]. These problems are named as "Path Planning". The difference between path following and path planning is that desired reference path is given or not given. Since we should follow the reference path, control inputs are constrained by path following task in this paper. Reference path is used with time optimal problem in Okajima et al [2004]. However, since this method treats trade-off between tracking error and moving time, the plant takes a shorter route for minimizing moving time. Therefore tracking error exists.

This paper is organized as follow: The problem is formulated in section 2. In particular, the classes of the desired reference paths and the state equation of the plants are shown. A constraint for following the path is derived in section 3. The optimal control problem is presented based on the constraint in section 4. At the last, the effectiveness of the method are shown by numerical examples with an automobile model.

### 2. PROBLEM FORMULATION

#### 2.1 Desired reference paths

It is assumed that plants move in horizontal plane and a reference path is given in the plane. Suppose the reference

path is given as a function with respect to the path length  $s$ , i.e., the reference path is represented as  $P_r(s) = (\xi_r(s), \eta_r(s))^T$ . In particular, we also assume  $\xi_r(s)$  and  $\eta_r(s)$  belong to class  $C^3$ .

$\Sigma$  is inertial coordinate and orthonormal bases of  $\Sigma$  is defined as  $e_1, e_2$  (See Fig. 1).  $P_r(s)$  is written as follow:

$$P_r(s) = \xi_r(s)e_1 + \eta_r(s)e_2 \quad (1)$$

Then, the curvature  $\kappa_r$  of each point  $s$  in reference path is represented by

$$\kappa_r(s) = \frac{d\theta_r(s)}{ds}. \quad (2)$$

Since  $\xi_r(s)$  and  $\eta_r(s)$  belongs to class  $C^3$ ,  $\kappa_r$  is differentiable in each  $s$ .

### 2.2 Characteristics of Plants

We consider path following control for a plant which is given by the following non-linear state equation:

$$\dot{x}_p(t) = f_{p1}(x_p(t)) + f_{p2}(x_p(t))u(t), \quad (3)$$

where  $x_p(t) \in R^n$  is state and  $u(t) = [u_1(t), \dots, u_m(t)]^T \in R^m$  is control input.  $\{ \cdot \}$  is the differential operator with respect to  $t$ . To divide tracking control and velocity control, we suppose  $m$  is greater than 2. Velocity of the plant  $v \in R$  and curvature of the plant  $\kappa$  are written as follow:

$$v(t) = h_1(x_p(t), u(t)), \quad (4)$$

$$\kappa(t) = h_2(x_p(t), u(t)). \quad (5)$$

In addition, we assume the velocity of the plant is not dependent on  $u(t)$  explicitly. i.e., (4) is written by  $v(t) = h_1(x_p)$ . In addition,  $h_2(x_p(t), u(t))$  is given as follow:

$$h_2(x_p(t), u(t)) = h_{21}(x_p(t)) + h_{22}(x_p(t))u_1(t), \quad (6)$$

where  $h_{22}(x_p) \neq 0$  holds. We should pay attention that many plants satisfy these conditions. For example, car with nonholonomic constraint, basic automobile model based on slip angle (Abe [1979]).

By using  $\kappa(t)$  and  $v(t)$ , we can calculate gravity of the plant in each time. Therefore, we can see that  $v(t)$  and  $\kappa(t)$  play a significant role in path following.

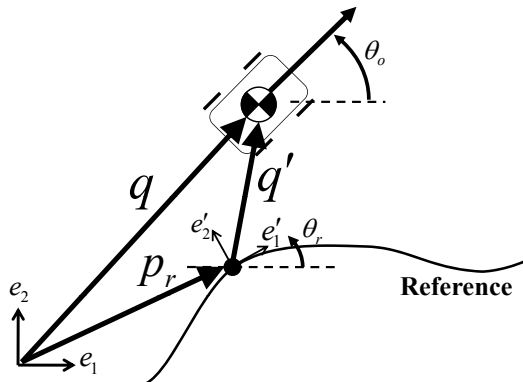


Fig. 1. Relative position of the reference path and the plant

### 3. CONTROL LAW FOR PATH FOLLOWING

Path following is achieved by appropriate  $u_1(t)$  in this paper. In what follows, we will show the control law for following the reference path asymptotically.

At the beginning, positional relationship between the plant and a point  $P_r(s)$  on the reference path is considered.

When the value of  $s$  is time varying, position of the point  $P_r(s(t))$  also moves.

In this paper,  $\zeta$  is defined as follow:

$$\zeta(q', s) = \text{sgn}(q' \cdot e'_2(s)) \|q'\|, \quad (7)$$

where  $\| \cdot \|$  shows Euclidean norm. Absolute value of  $\zeta$  indicates length of  $q'$ . Sign of  $\zeta$  indicates  $e'_2$  element of  $q'$ . i.e., if  $\zeta$  is positive, the plant exists in left half plane of  $e'_1$  axis.

Former relations are satisfied for any given  $s(t)$ . Moreover, we consider a special point  $s = s_r$  which orthogonalize  $q'$  and  $e'_1$  (Altafani [2002], Okajima et al [2004]). Then such  $P_r(s_r)$  is named as "reference point" (See Fig. 2). I.e.,  $s_r(t)$  represent the dynamics of reference point when the following equation holds for any  $t$ .

$$q'(t) \cdot e'_1(s_r(t)) = 0 \quad (8)$$

If (8) holds in initial state, we can consider  $s_r(t)$  by the following state equation (See Altafani [2002]):

$$\dot{x}(t) = F(x(t), u(t)), \quad x = [x_p^T, x_{re}^T]^T \quad (9)$$

$$F(x, u) = \begin{bmatrix} f_{p1}(x_p) + f_{p2}(x_p)u \\ h_1(x_p)h_2(x_p, u) - \hat{\kappa}_r \frac{h_1(x_p) \cos \theta}{1 - \hat{\kappa}_r z} \\ \frac{h_1(x_p) \cos \theta}{1 - \hat{\kappa}_r z} \\ h_1(x_p) \sin \theta \end{bmatrix}$$

where  $x_{re} = [\theta, s_r, z]^T$ . (9) includes (3), (4) and (5). We can see that  $z$  indicates signed distance from the plant and the reference point. Therefore, the plant follows the reference path exactly when  $z(t) = 0$  holds. Then, we will consider a control law to satisfy the following equation instead of path following task:

$$\lim_{t \rightarrow \infty} z(t) = 0. \quad (10)$$

To achieve (10),  $z(t)$  is used as output in output zeroing method. When  $s^2 + a_1s + a_0$  is given as Hurwitz polynomial, the following equation:

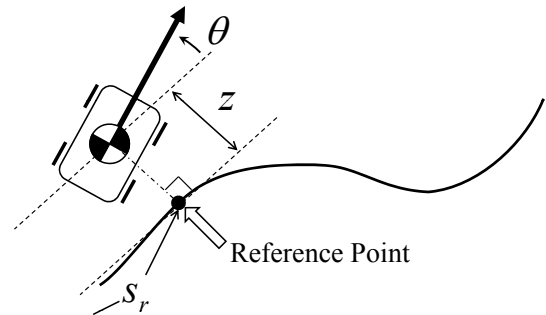


Fig. 2. Characteristics of reference point

$$\frac{d^2 z}{dt^2} + a_1 \frac{dz}{dt} + a_0 z = 0 \quad (11)$$

enable us to satisfy equation (10). On the other hand,  $d^2 z/dt^2$  of (9) can be written as a linear function of  $u_1$ . Therefore, we can write  $u_1$  by a function of  $x$  and  $\tilde{u} = [u_2, \dots, u_m]^T$  by explicit form when the following statement holds:

$$h_1(x_p)^2 \cos \theta h_{22}(x_p) + \sin \theta \frac{\partial h_1}{\partial x_p} f_{p2}(x_p) \underbrace{[1, 0, \dots, 0]^T}_m \neq 0. \quad (12)$$

Since we had already assumed  $h_{22} \neq 0$  in section 2, (12) holds when  $v \neq 0$  and second term of (12) closes to zero. The second term is small when  $\theta$  is small and the term is zero when  $u_1$  gives no impact on  $dv/dt$  directly.

Consequently,  $u_1$ , given by (11), is used for path following. When the  $u_1$  is substituted for (9), we obtain the following state equation:

$$\begin{aligned} \dot{x} &= \tilde{F}(x(t), \tilde{u}(t)) \\ &= \tilde{F}_1(x) + \tilde{F}_2(x)\tilde{u}, \end{aligned} \quad (13)$$

where the state of (13) is same as that of (9). When the plant dynamics according to (13), it is clear that the plant follows the reference path asymptotically for any time series of  $\tilde{u}(t)$ . In turn, (11) can be considered as constraint for following the path. Then optimal  $\tilde{u}(t)$  is derived in next section.

#### 4. OPTIMAL CONTROL PROBLEM

To consider the optimal control problem, the cost function  $J$  is defined as follow:

$$J = J_u + J_t, \quad (14)$$

where  $J_u$  and  $J_t$  are amplitude of control input and reaching time from start to end point of the desired reference path, respectively.  $\ell$  is interval for cost function (See Fig. 3).

Let (3),(4),(5) and initial position  $q(t_0)$  be given. Furthermore, initial angle  $\theta_o(t_0)$ , initial states  $x_p(t_0)$  and desired reference path  $p_r(s)$  also be given.  $s_r(t_0) = s_{r0}$  and  $\theta_r(t_0)$  are decided uniquely when designer choose a point which satisfy (8). Consequently, initial states of (13) are given by

$$x(t_0) = \begin{bmatrix} x_{p0} \\ \theta_o(t_0) - \theta_r(s_{r0}) \\ s_{r0} \\ \zeta(q'(t_0), s_{r0}) \end{bmatrix}. \quad (15)$$

Then  $J_u$  and  $J_t$  are determined as follows by using interval  $[s_{r0}, s_{r1}]$  with  $s_{r1} = s_{r0} + \ell$ .

$$J_u = \int_{t(s_{r0})}^{t(s_{r1})} D_{u_1}(u_1(x)) + D_{\tilde{u}}(\tilde{u}) dt \quad (16)$$

$$J_t = g(t(s_{r1}) - t(s_{r0})) = \int_{t(s_{r0})}^{t(s_{r1})} g dt \quad (17)$$

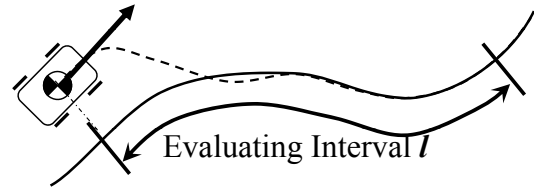


Fig. 3. Evaluating interval

We should pay attention that  $D_u(u)$  is differentiable with respect to each component of  $u$ . For example,  $u^T u$  is suitable as  $D_u(u)$ .  $t(s_{r1})$  of (17) represent the reaching time to the end point of the interval. On the other hand, second term of (17) is the cost for evaluating time. In the result, The proposed method can be summarized as the following optimal control problem.

*Problem 1.* Find  $\tilde{u}$  which minimize:

$$J = \int_{t(s_{r0})}^{t(s_{r1})} D_{u_1}(u_1(x)) + D_{\tilde{u}}(\tilde{u}) + g dt, \quad (18)$$

subject to (13), (15).

The aim of this paper “velocity control in path following” can be treated by *problem 1*. This problem belongs to standard optimal control problem.

The difference between proposed method and Okajima et al [2004] is as follow. Okajima et al [2004] uses cost function of  $z$  to follow the reference path. The proposed method use  $u_1(t)$  with (11) as constraint for asymptotical path following.

In the next section, numerical examples would be shown for examining the effectiveness. *Problem 1* can be reduced to two point boundary value problem. The solutions of the two point boundary value problem are obtained by MATLAB (bvp4c.m).

In what follows, notations about two point boundary value problem are written. The Lagrangian function for deriving the problem is as follow:

$$L = D_{u_1}(u_1(x)) + D_{\tilde{u}}(\tilde{u}) + g + \lambda^T (\tilde{F}(x, \tilde{u}) - \dot{x}), \quad (19)$$

where  $\lambda \in R^n$  is called as costate. Costate equation is derived by

$$\frac{\partial L}{\partial x} - \frac{d}{dt} \left( \frac{\partial L}{\partial \dot{x}} \right) = 0 \quad (20)$$

The two point boundary value problem is consist of state equation, costate equation and boundary conditions (initial states etc.).

When  $D_{\tilde{u}}(\tilde{u})$  is given as quadratic form, i.e.,

$$D_{\tilde{u}}(\tilde{u}) = \tilde{u}^T Q \tilde{u}, Q > 0 \quad (21)$$

holds,  $\tilde{u}$  is given by

$$\tilde{u}(t) = -\frac{1}{2} Q^{-1} \tilde{F}_2(x)^T \lambda. \quad (22)$$

We can obtain  $\tilde{u}(t)$  by  $\lambda(t)$  which is given by solving two point boundary value problem. Since  $u_1(t)$  has already been given by (11), we can obtain  $u(t)$ .

In this two point boundary value problem, the terminal time is free. When we want to obtain numerical solution of  $u(t)$  by `bvp4c.m`, terminal time should be fixed. In this paper, this problem is reduced to two point boundary value problem with fixed terminal time by idea of the “time-state control method ( Sampei et al [1986] ) ” with  $\tau(x) = s_r$ .

### 5. NUMERICAL EXAMPLES

To examine the effectiveness of the proposed method, the following automobile model is used as a plant. The model has two input (steer-angle  $\delta(t)$  and acceleration/deceleration  $w(t)$ ). The details of the plant are shown in Appendix.

$$\dot{x}_p(t) = f_p(x_p(t), u(t)), \quad (23)$$

$$x_p = [\beta \quad \dot{\psi} \quad v]^T, \quad u = [\delta \quad w]^T$$

$$f_p(x_p, u) = \begin{bmatrix} \frac{a_{11}}{v}\beta + (-1 + \frac{a_{12}}{v^2})\dot{\psi} + \frac{a_{13}}{v}\delta \\ a_{21}\beta + \frac{a_{22}}{v}\dot{\psi} + a_{23}\delta \\ a_{31}(v - v_0) + a_{32}w \end{bmatrix}, \quad (24)$$

where  $a_{ij}$  are coefficients of automobile model. The following values are used for numerical examples.

$$\begin{bmatrix} a_{11} & a_{12} & a_{13} \\ a_{21} & a_{22} & a_{23} \end{bmatrix} = \begin{bmatrix} -43 & -109 & 18 \\ 5.45 & -34.09 & 10.8 \end{bmatrix}$$

$$\begin{bmatrix} a_{31} \\ a_{32} \end{bmatrix} = \begin{bmatrix} -0.5 \\ 2 \end{bmatrix}, \quad v_0 = 5$$

Then the velocity and the curvature of the automobile model are written as follow:

$$h_1(x_p, u) = [0 \ 0 \ 1]x_p, \quad (25)$$

$$h_2(x_p, u) = \frac{a_{11}}{v(t)^2}\beta(t) + \frac{a_{12}}{v(t)^3}\dot{\psi}(t) + \frac{a_{13}}{v(t)^2}\delta(t). \quad (26)$$

We can see that when  $\delta$  of  $h_2(x_p, u)$  is ascribed as  $u_1$ , (26) satisfy (6). Moreover, if  $|v(t)|$  is large in (26),  $\kappa(t)$  is less affected by  $\delta(t)$ . We have to input large  $\delta$  to turn for high velocity automobile. Therefore, the plant has trade-off between magnitude of  $\delta$  and moving time.

The following  $J$  is used as the cost function:

$$J = \int_{t(s_{r0})}^{t(s_{r1})} g_1\delta(x)^2 + g_2w^2 + g_3dt \quad (27)$$

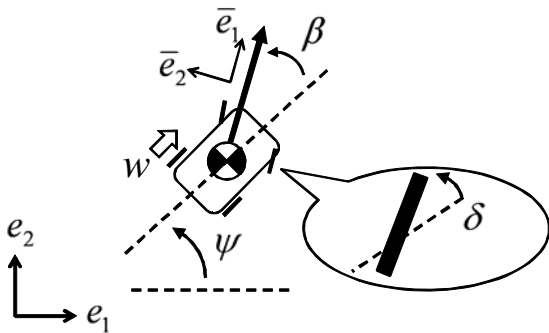


Fig. 4. Automobile model

The problem in this example is to minimize  $J$  by  $w(t)$ . We can expect that we obtain  $w(t)$  which satisfies small control input  $\delta(t)$  by large  $g_1$  and short reaching time by large  $g_3$ . We choose  $g_1 = 150$ ,  $g_2 = 1$  for all examples. Two types of reference path are used for numerical example. To analyze the effectiveness of weights, reference path of simple to understand would be used in Case 1. More complex path would be used in Case 2.

- Case 1

The following  $\kappa_r(s_r)$  with  $x_r(0) = 0$ ,  $y_r(0) = 0$ ,  $\theta_r(0) = 0$  is used as the reference path in Case 1(See Fig. 5):

$$\kappa_r = 0, \quad 0 \leq s_r < 12,$$

$$\kappa_r = 0.04(1 - \cos(0.15s_r - 1.8)), \quad 12 \leq s_r.$$

The path is simple to understand the impact for the cost. In straight line part, the reader would assume acceleration is better for minimizing the cost. On the other hand, the reader would assume deceleration is better in curve part. Initial states  $x(0)$  of numerical examples are chosen as zero except velocity ( $v(0) = 10$ ).

First, we show the case of changing weight  $g_3$ . Fig. 6 shows the velocity and Fig. 7 shows time-series of the steer input. Solid line shows the case  $g_3 = 100$ , dashed line shows the case  $g_3 = 50$ , dotted line shows the case  $g_3 = 20$ , dash-dotted line shows the case  $g_3 = 0$ . We can see that the automobile's velocity is high when  $g_3$  is large value. In particular, the automobile with  $g_3 = 100$  is accelerated in straight line part. However, the automobile with  $g_3 = 0$  is decelerated in spite of the same part of the reference path. In Fig. 7, we can see that large steer input is required when  $g_3$  is large. By each control inputs, reaching time is 2.01[s], 2.35[s], 2.81[s], 3.54[s], respectively, in Fig. 7. We can see from this figure that reaching time is short when  $g_3$  is large. Trade-off between control inputs and reaching time have been treated in the proposed method. Note that since  $z(0) = 0$  and  $\theta(0) = 0$  hold, automobiles follow the reference path strictly in Case 1.

Then we compare the proposed method to a constant velocity case.  $g_3$  is choose by trial and error for easily comparison. We obtain  $g_3 = 12.35$  which satisfy same reaching time as the case of constant velocity ( $v = 10$ ). Figs. 8, 9 show the velocities and steer angles. Dashed line shows the case of constant velocity, solid line shows the case of proposed method. Horizontal axis of Fig. 8 is  $s_r$ . We can see that the velocity of proposed method is

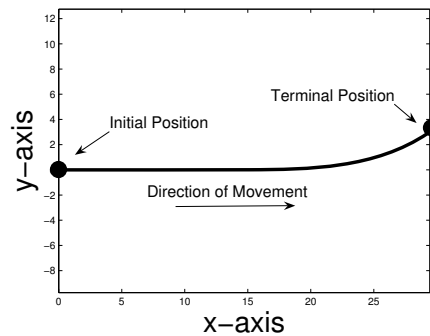


Fig. 5. reference path and automobile's trajectory

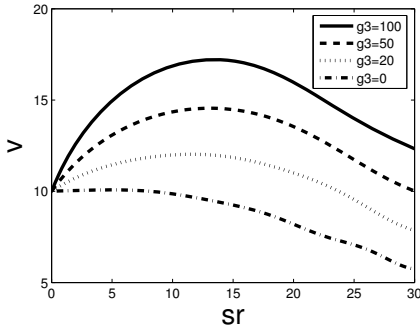


Fig. 6. Velocities for each weights

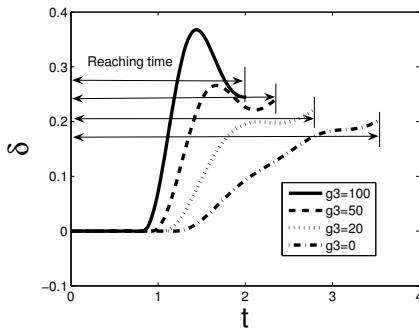


Fig. 7. Steer angles for each weights

large in straight line part and velocity is small in curve. Horizontal axis of Fig. 9 is time  $t$ . We can confirm the reaching time is same ( 3[s] ) by Fig. 9. In this figure, we can see that steer angle  $\delta(t)$  of proposed method is smaller in spite of other conditions (conditions: reaching time and automobile's trajectory are same). Actually,

$$J_{\delta} = \int_{t(s_{r0})}^{t(s_{r1})} g_1 \delta(t)^2 dt \quad (28)$$

of the proposed method (  $J_{\delta} = 6.55$  ) is smaller than that of constant velocity case (  $J_{\delta} = 9.27$  ).

Table 1 shows  $J$  of proposed method and that of constant velocity for some  $g_3$ . Note that since  $g_1$  and  $g_2$  are fixed value,  $J_u$  for constant velocity can be calculable as  $J_u = 13.96$ . Now therefore values of  $J$  of constant velocity case are given by  $J = 13.96 + g_3 \times 3$ . On the other hand, control inputs (Numerical solutions) are different in each weights of the proposed method. We can see from Table 1 that values of the proposed method are smaller than that of constant velocity for all  $g_3$ .

Table 1. Values of the cost function

method - $g_3$	100	50	20	0	12.35
Proposed method	$J=256.54$	$J=147.15$	$J=71.31$	$J=8.18$	$J=49.31$
The case of $v(t) = 10$	$J=313.96$	$J=163.96$	$J=73.96$	$J=13.96$	$J=51.01$

• Case 2

Results of various  $z(0)$  are shown in Case 2. The following  $\kappa_r(s_r)$  with  $x_r(0) = 0, y_r(0) = 0, \theta_r(0) = 0$  is used as the reference path:

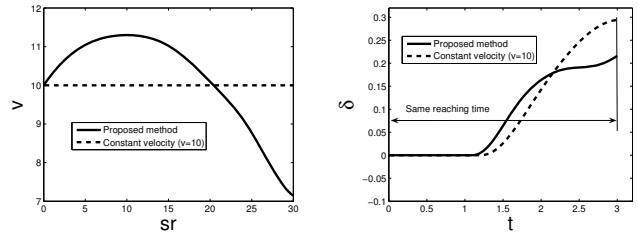


Fig. 8. Velocities of the proposed method and constant case

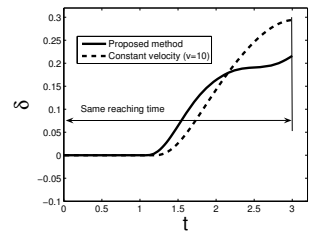


Fig. 9. Steer angles of the proposed method and constant case

$$\kappa_r = 0.06 \cos(0.1s_r) \quad (29)$$

$\kappa_r$  is positive in  $s_r < 2.5\pi$  and negative in other area. We also use  $v(0) = 10$  for this example. Other initial states are chosen as zero.  $g_3 = 30$  for the

The examples of  $z(0) = -2$ (thick,dashed),  $-1$ (thin,dashed),  $0$ (thick,solid),  $1$ (thin,dash-dotted),  $2$ (thick,dash-dotted) are shown in Figs. 10, 11. We can see that each automobile tracks to the reference path asymptotically in Fig. 10. We obtain various series of velocities in Fig. 11. In particular, complex time series of  $v$  are obtained for  $z(0) = 1, 2$ .  $J$  of each  $z(0)$  are given as 238.6, 141.1, 107.9, 150.8, 274.9. Cost values are asymmetric for  $z(0)$  because of the form of the reference path.

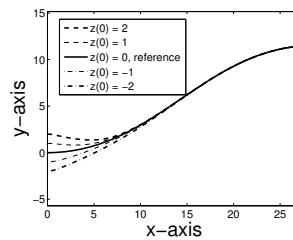


Fig. 10. trajectories of automobile and reference path for different  $z(0)$

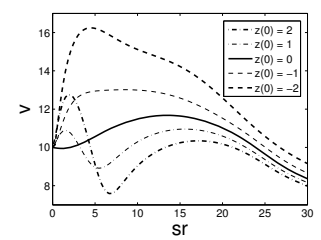


Fig. 11. velocities of automobile for different  $z(0)$

6. CONCLUSIONS

In this paper, we have proposed the method which achieve velocity control and path following. Proposed method is based on optimal control problem. Path following task is treated as a constraint for the problem. By using the constraint, we can treat two tasks (appropriate velocity control and path following) as standard optimal control problem. Minimization of the cost function enable us to treat trade-offs between control input and reaching time. The effectiveness of proposed method has been shown by numerical examples of automobile model.

Since the proposed method is given as standard optimal control problem, it is expected that we apply the proposed method to more complex plants such as aircraft with many inputs.

REFERENCES

M. Sampei and T. Itoh. Path Planning and Path Tracking Control of Wheeled Vehicles Using Nonlinear System Theory -Parking Control Using Forward and Backward

- Movement. *Transactions of The Institute of Systems, Control and Information Engineers*, volume 6, pages37–47, 1993.
- M. Sampei, T. Tamura, T. Kobayashi and N. Shibui. Arbitrary Path Tracking Control of Articulated Vehicles Using Nonlinear Control Theory. *IEEE Transactions on Control Systems Technology*, volume 3, pages125–131, 1995
- C. Altafini. Following a path of varying curvature as an output regulation problem. *IEEE Transactions on Automatic Control*, volume 47, pages1551–1556, 2002.
- D. Soetanto, L. Lapierre and A. Pascoal. Adaptive, non-singular path-following control of dynamic wheeled robots. *Proceeding of the 42nd IEEE Conference on Decision and Control*, pages1765-1770, 2003.
- I. Kammer, O. Yakimenko, A. Pascoal and R. Ghabche-loo. Path Generation, Path Following and Coordinated Control for Time Critical Missions of Multiple UAVs *Proceedings of the 2006 American Control Conference*, pages4906–4913, 2006.
- V. Rajan. Minimum time trajectory planning. *IEEE Transactions on Robotics and Automation. Proceedings*. pages759–764, 1985.
- Y. Chen and A. A. Desrochers. A near-minimum time controller for two coordinating robots grasping an object. *Proceedings of Robotics and Automation*, pages1184–1189, 1989.
- M. Galicki. Time-Optimal Controls of Kinematically Redundant Manipulators with Geometric Constraints. *IEEE Transactions on Robotics and Automation*, pages89–93, 2000.
- D. Casanova, R. S. Sharp and P. Symonds. Technical Note: Construction of race circuit geometry from on-car measurements. *Proc. I. Mech. E., Journal of Automobile Engineering*, 215(D9), pages1033–1042, 2001.
- K. Pathak, J. Franch and S. K. Agrawal Velocity and Position Control of a Wheeled Inverted Pendulum by Partial Feedback Linearization. *IEEE Transactions on Robotics*, volume 21, pages505–513, 2005.
- H. Okajima and T. Asai. Path-Following Control based on Trajectory Differences. *Proc. of the 10<sup>th</sup> IFAC/IFORSIMACS/IFIP symposium on large scale systems: theory and applications*. pages735–740, 2004.
- M. Sampei and K. Furuta. On Time Scaling for Nonlinear Systems: Application to Linearization. *IEEE Transactions on Automatic Control*, volume 31, pages459–463, 1986.
- M. P. do Carmo. Differential Geometry of Curves and Surfaces. *Prentice-Hall*, 1976.
- M. Abe. Vehicle Dynamics and Control. *Kyo-ritsu Publishing*. 1979.
- F. L. Lewis and V. L. Syrmos. Optimal Control. *A Wiley-Interscience Publication*, 1995.
- A. Isidori. Nonlinear Control Systems. *Springer*, 1995.

## Appendix A. AUTOMOBILE MODEL

The automobile model is derived as follow: To describe the dynamics of the automobile, a reference frame for the automobile is set such that one basis vector  $\bar{e}_1(t)$  is along the velocity vector, while another basis vector  $\bar{e}_2(t)$  is orthogonal to  $\bar{e}_1(t)$  (Fig. 4). Note that those basis vectors have unit length and that they are time-varying because of the motion of the automobile.

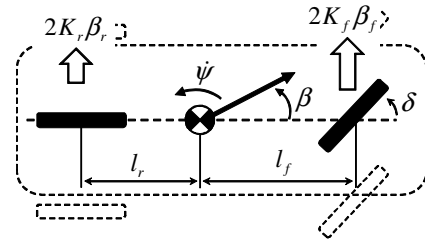


Fig. A.1. slip angles of front and rear tires

The velocity vector and the force vector of the automobile are represented as follows:

$$\tilde{v} = v_{\bar{e}_1}(t)\bar{e}_1(t) + v_{\bar{e}_2}(t)\bar{e}_2(t), \quad (\text{A.1})$$

$$\tilde{f} = f_{\bar{e}_1}(t)\bar{e}_1(t) + f_{\bar{e}_2}(t)\bar{e}_2(t), \quad (\text{A.2})$$

where  $\tilde{v}$  and  $\tilde{f}$  are the velocity and the force vectors, respectively, and  $v_{\bar{e}_1}$ ,  $v_{\bar{e}_2}$ ,  $f_{\bar{e}_1}$ ,  $f_{\bar{e}_2}$  are elements. By the definition of  $\bar{e}_1(t)$  and  $\bar{e}_2(t)$ ,  $v_{\bar{e}_2} = 0$  holds for any  $t$ .

By considering the rotation of the coordinate frame, the equations of motion are given as follow:

$$m(\dot{v}_{\bar{e}_1}(t) - v_{\bar{e}_2}(t)(\dot{\psi}(t) + \dot{\beta}(t))) = f_{\bar{e}_1}(t), \quad (\text{A.3})$$

$$m(\dot{v}_{\bar{e}_2}(t) + v_{\bar{e}_1}(t)(\dot{\psi}(t) + \dot{\beta}(t))) = f_{\bar{e}_2}(t), \quad (\text{A.4})$$

$$I\dot{\psi}(t) = M(t), \quad (\text{A.5})$$

where  $m$  is the mass of the automobile,  $I$  is the moment of inertia,  $M$  is the total torque of the center of gravity,  $\dot{\psi}$  is the yaw rate and  $\beta$  is the angle between the orientation of the automobile and the velocity vector (Fig. 4). Since  $v_{\bar{e}_2} = 0$  holds,  $v_{\bar{e}_2}$  and  $\dot{v}_{\bar{e}_2}$  of (A.3) and (A.4) are zero, respectively. For simplicity, we describe  $v_{\bar{e}_1}$  as  $v$ .

In this paper,  $f_{\bar{e}_1}$  is assumed to be given by damping force  $\mu(v - v_0)$  and driving force  $w$ . Then (A.3) is written by the following equation:

$$m\dot{v}(t) = \mu(v(t) - v_0) + w(t) \quad (\text{A.6})$$

where  $v_0$  is the operating point of the velocity.

Moreover, we assume the side forces are generated due to the slip angles of each tire (See Fig. A.1, such assumption is also used in Abe [1979]). The each forces are given by  $K_f\beta_f(t)\bar{e}_2(t)$  and  $K_r\beta_r(t)\bar{e}_2(t)$  where  $K_f$  and  $K_r$  are the cornering powers of the front and the rear tires respectively, and  $\beta_f(t)$  and  $\beta_r(t)$  are the slip angles (angle from orientation of each tire to velocity vector). Furthermore,  $\beta_f(t)$  and  $\beta_r(t)$  can be approximated by

$$\beta_f(t) = \beta(t) + \frac{l_f\dot{\psi}(t)}{v(t)} - \delta(t), \quad (\text{A.7})$$

$$\beta_r(t) = \beta(t) - \frac{l_r\dot{\psi}(t)}{v(t)}, \quad (\text{A.8})$$

where  $l_f$  and  $l_r$  are the distances from the center of gravity to the positions of the front and the rear tires. Then the following equations hold:

$$f_{\bar{e}_2}(t) = 2K_f\beta_f + 2K_r\beta_r, \quad (\text{A.9})$$

$$M(t) = -2K_f l_f \beta_f + 2K_r l_r \beta_r. \quad (\text{A.10})$$

By (A.4),(A.5),(A.6),(A.9) and (A.10), we obtain (23) as the state equation of the automobile.